

Cambridge University Press

978-1-107-41378-8 - Materials Research Society Symposium Proceedings: Volume 540:
Microstructural Processes in Irradiated Materials

Editors: Steven J. Zinkle, Glenn E. Lucas, Rodney C. Ewing and James S. Williams

Excerpt

[More information](#)

Part I
Semiconductors

Cambridge University Press

978-1-107-41378-8 - Materials Research Society Symposium Proceedings: Volume 540:
Microstructural Processes in Irradiated Materials

Editors: Steven J. Zinkle, Glenn E. Lucas, Rodney C. Ewing and James S. Williams

Excerpt

[More information](#)

Cambridge University Press

978-1-107-41378-8 - Materials Research Society Symposium Proceedings: Volume 540:

Microstructural Processes in Irradiated Materials

Editors: Steven J. Zinkle, Glenn E. Lucas, Rodney C. Ewing and James S. Williams

Excerpt

[More information](#)

MICROSTRUCTURE EVOLUTION IN LOW-TEMPERATURE, ION-IMPLANTED $\text{Al}_x\text{Ga}_{1-x}\text{As}$

B. W. LAGOW*, I. M. ROBERTSON*, L. E. REHN**, and J. J. COLEMAN*

* Frederick Seitz Materials Research Laboratory, University of Illinois at Urbana-Champaign, Urbana IL 61801, b-lagow@uiuc.edu

** Materials Science Division, Argonne National Laboratory, Argonne IL 60439

ABSTRACT

The accumulation of ion implantation damage in $\text{Al}_x\text{Ga}_{1-x}\text{As}$ / GaAs heterostructures ($0 \leq x \leq 0.85$) at 77 K has been investigated by using a combination of RBS (at 77 K and 293 K) and TEM (at 293 K). Recovery, as seen by a decrease in the channeling yield, occurs on warming to room temperature unless the material has been driven amorphous or $x \geq 0.85$. Depending on the implantation condition, the recovered structure consists of either planar defects or dislocation loops. Planar defects were also observed in alloys with $x = 0.85$, although they were confined to a narrow band that separated the amorphous from the crystalline material. By implanting with ions of different energy it was shown that amorphization can initiate within the layer away from the interfaces, showing that interfaces are not needed for amorphization. Implantations with 500 keV Kr ions were performed at 50 K *in-situ* in the Intermediate-Voltage Electron Microscope -- Accelerator facility at Argonne National Laboratory. Planar defects were produced on warmup, showing that they are not necessary for amorphization. We propose that amorphization initiates because of an accumulation of damage and that the dependence of the amorphization dose on Al content is related to differences in cascade dynamics.

INTRODUCTION

The evolution of ion damage in $\text{Al}_x\text{Ga}_{1-x}\text{As}$ / GaAs heterostructures has been investigated extensively [1-7], but with no unified mechanism emerging to explain the amorphization process or dependence of amorphization dose on Al content. This is in part due to the difficulty in assessing all the data, as different implantation temperatures, ion masses and energies, sample geometries and compositions have been employed. In addition, in many studies the samples were implanted at 77 K, but analyzed at room temperature, which assumes that no recovery of the microstructure occurs during warmup [1-5]. This assumption is, however, not always justified. For specific implantation conditions, the damage in both GaAs and AlAs has been found to recover when they are warmed above ~200K [8-11]. Despite these difficulties there are a number of aspects about the damage evolution in $\text{Al}_x\text{Ga}_{1-x}\text{As}$ on which there is general agreement:

1. For a given ion mass and energy, the ion dose required to amorphize $\text{Al}_x\text{Ga}_{1-x}\text{As}$ at a given implant temperature increases with Al content [3-7]. This is shown in Figure 1 for different ion implantation conditions; the amorphization dose was taken as the dose at which the channeling yield first coincides with that of the random. Clearly, the dose to amorphize GaAs is lower than that of AlAs by up to three orders of magnitude.

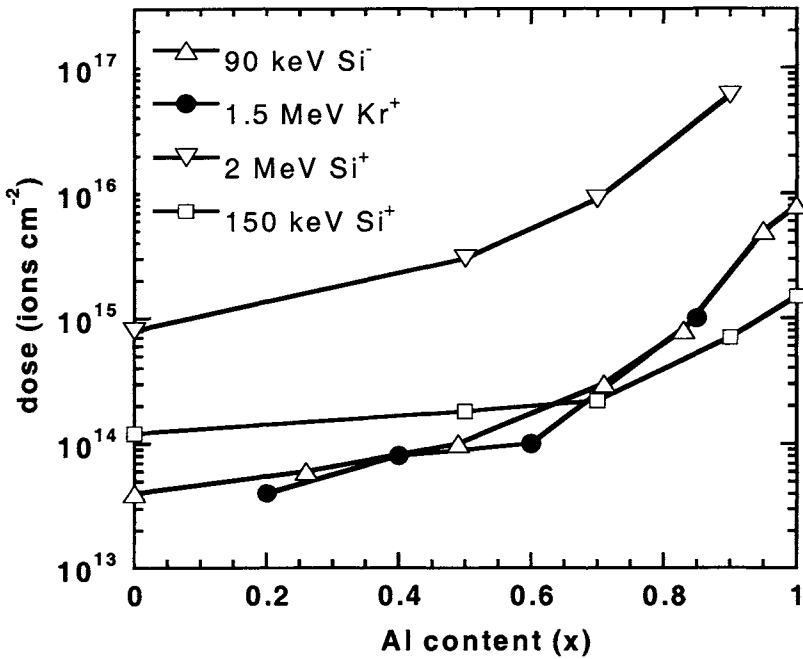


Figure 1: Dose to amorphization at 77 K as a function of Al content. Data from [3,5-7].

2. The rate of accumulation of damage increases with depth regardless of sample composition in implant conditions in which the end-of-range is well beyond the back interface. The distribution of damage in a 80 nm GaAs / 320 nm Al_{0.6}Ga_{0.4}As / GaAs sample implanted at 77 K with 1.5 MeV Kr ions to a dose of 10¹⁴ ions cm⁻² is shown in Figure 2, in which the low and room temperature channeling data and room temperature electron micrographs from different depths in the cross-sectional sample are presented [6]. The 77 K channeling yield from the sample increases with depth. The damage observed in the electron micrographs, Figures 2a-c, can only be compared to the room temperature channeling spectra, because recovery, as evidenced by a decrease in the channeling yield, occurs on warmup. The upper GaAs/Al_{0.6}Ga_{0.4}As interface is intact, although rougher than in unimplanted material. The upper portion of the Al_{0.6}Ga_{0.4}As layer is crystalline, but contains planar defects that increase in density with depth (Figure 2a and 2b). At a depth of approximately 220 nm, isolated amorphous regions exist within defective crystalline material (Figure 2c). The density of amorphous regions increases with further increase in depth until a continuous amorphous layer forms. Within the amorphous layer, small isolated crystalline regions containing planar defects are observed. The orientation of these planar defects is the same as in crystalline material, suggesting that the crystallites are remnants of the parent material rather than regions that have formed because of continued implantation. These changes in microstructure are consistent with the room temperature channeling yields, and show that a continuous amorphous layer is stable against warmup.

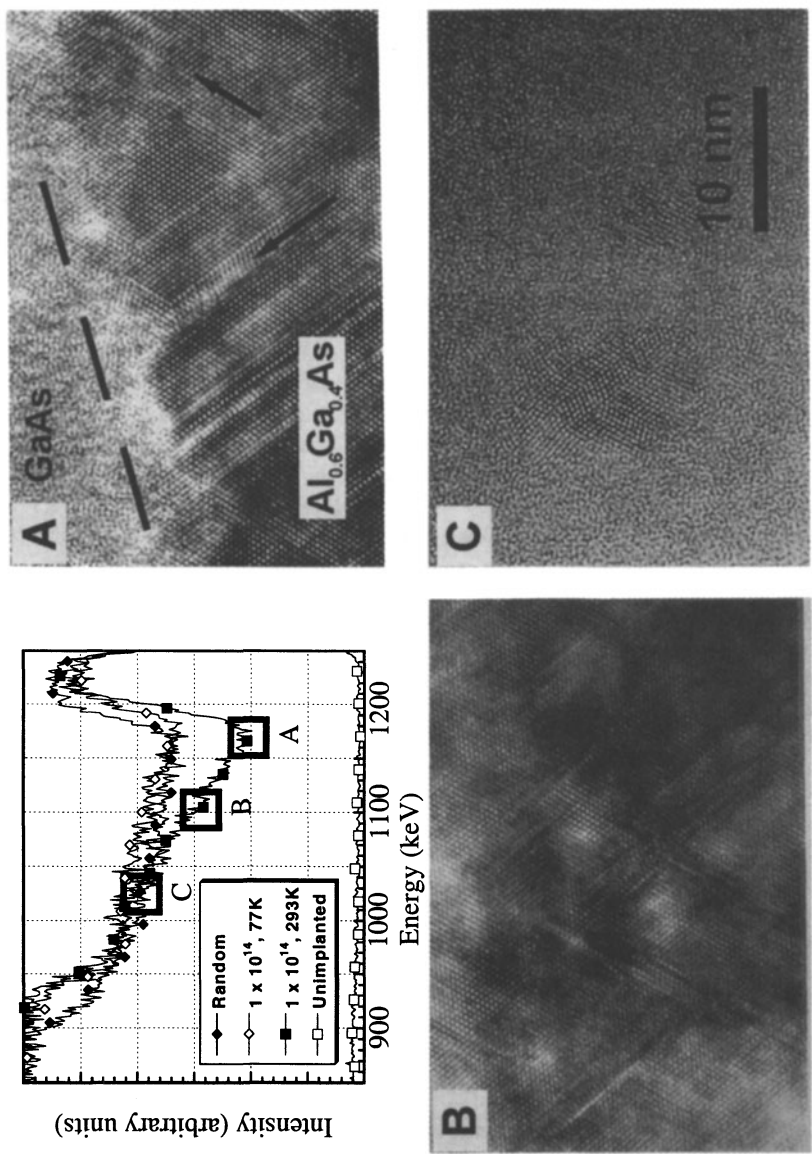


Figure 2: RBS and high-resolution TEM for $\text{Al}_{0.6}\text{Ga}_{0.4}\text{As}$ sample implanted at 77 K with 1.5 MeV Kr to a dose of 10^{14} ions cm^{-2} . Dashed line in (A) roughly corresponds to upper interface. Images from approximate depths into layer of A) 0 nm, B) 100 nm, C) 220 nm. From ref. [6].

Cambridge University Press

978-1-107-41378-8 - Materials Research Society Symposium Proceedings: Volume 540:
Microstructural Processes in Irradiated Materials

Editors: Steven J. Zinkle, Glenn E. Lucas, Rodney C. Ewing and James S. Williams

Excerpt

[More information](#)

3. Intermixing occurs at the interfaces. For high-energy ion implants into samples with shallow buried $\text{Al}_x\text{Ga}_{1-x}\text{As}$ layers, intermixing is greater at the deeper than the shallower interface. Klatt *et al.* [4] reported values for the mixing efficiency of $250 \text{ \AA}^5 \text{ eV}^{-1}$ and $440 \text{ \AA}^5 \text{ eV}^{-1}$ for the shallow and deep interface, respectively, in structures with a 100 nm AlAs layer buried in GaAs and implanted at 80 K with 1.0 MeV Kr. TEM intensity profiles, which can be directly related to compositional profiles, across amorphous GaAs/ $\text{Al}_{0.6}\text{Ga}_{0.4}\text{As}$ show that following an implantation at 77 K with 1.5 MeV Kr to a dose of $10^{14} \text{ ions cm}^{-2}$, intermixing extends over about 6 nm [6].

Interfaces have also been described as having other effects on damage accumulation. For example, it has been suggested that interfaces act as nucleation sites for amorphization [2,3], afford protection to nearby GaAs [2], and are sinks and/or sources for defects [3]. This latter effect may be enhanced by the development of an electric field across the interface [1,4].

The change in damage accumulation with increasing Al content has led to different amorphization mechanisms being suggested for alloys containing low, medium, and high concentrations of Al. Tan *et al.* [5] have proposed that dynamic annealing occurs at 77 K and that it increases with aluminum content; in high Al content alloys ($x > 0.85$), increased dynamic annealing creates planar defects during implantation, which then act as precursors to amorphization. However, no mobile defects have been observed in AlAs [11] until temperatures above 200 K, no dose rate dependence of the amorphization has been reported for implantations at 77 K, and planar defects exist in lower Al content samples in which they do not appear to influence the amorphization [6]. Considering these points, it seems unlikely that dynamic annealing is active at 77 K, even in high Al content samples.

Turkot *et al.* [6] have proposed that amorphization is caused by the superposition of the distribution of energetic cascade events on a background of point defects. The variation of damage with depth is a result of the depth variation of energetic cascades (as determined using a modified version of TRIM [14], described elsewhere [6]). In other words, the amorphization process is related to the structure of the displacement cascade created as an energetic particle loses its energy. This mechanism agrees with the observed variation in depth of the damage distribution in $\text{Al}_{0.2}\text{Ga}_{0.8}\text{As}$, where amorphous regions can form by the direct impact mechanism [7], and is consistent with amorphization occurring first at the back of the layer. In this mechanism, the planar defects observed in the TEM are a consequence of recovery that occurs upon warming the sample to room temperature and are not important in the amorphization process. Also, under conditions in which either a low concentration of point defects or a low density of energetic cascades is created, amorphization will not occur. This was corroborated by a TEM study of $\text{Al}_{0.6}\text{Ga}_{0.4}\text{As}$ samples implanted at 77 K with 1.0 MeV Ar (which introduces a high variation in cascades but a low concentration of point defects), in which the microstructure consisted of dislocation loops.

In this paper we present the results of experiments designed to further test the mechanism proposed by Turkot *et al.* [6]. The range of sample composition has been extended to include alloys with $x = 0.6, 0.7, 0.8$, and 0.85 , and the ion implantations to include 700 keV and 1.5 MeV Kr. In addition, the damage evolution caused by a high-energy ion implantation at low temperature (50 K) has been investigated by performing the implantation and electron microscopy *in-situ* in the Intermediate-Voltage Electron Microscope (IVEM) -- Accelerator facility at Argonne National Laboratory.

Cambridge University Press

978-1-107-41378-8 - Materials Research Society Symposium Proceedings: Volume 540:
Microstructural Processes in Irradiated Materials

Editors: Steven J. Zinkle, Glenn E. Lucas, Rodney C. Ewing and James S. Williams

Excerpt

[More information](#)

EXPERIMENTAL PROCEDURE

The geometry of the specimens used was either 80 nm GaAs / 320 nm $\text{Al}_x\text{Ga}_{1-x}\text{As}$ / GaAs or 80 nm GaAs / 2-3 μm $\text{Al}_x\text{Ga}_{1-x}\text{As}$ / GaAs; the latter geometry was used exclusively for the *in-situ* TEM experiments. Off-axis implantations were performed at 77 K with 700 keV or 1.5 MeV Kr on bulk samples with $x=0.6, 0.7, 0.8$, or 0.85 . In addition, some samples were implanted sequentially with 3.0 MeV Kr and then with 1.5 MeV Kr. Following implantation, Rutherford backscattering channeling spectra were collected first at 77 K and again at 293 K after the sample was allowed to warmup overnight. *In-situ* TEM implantations were performed at 50 K with 500 keV Kr.

RESULTS

The RBS channeling plots showing accumulation of damage at 77 K as a function of ion dose are presented in Figures 3a-c for samples with $x = 0.7, 0.8$, and 0.85 and in Figure 2 for $x = 0.6$ [6]. For each alloy, the channeling yield approaches that of the random, although the amorphization dose increases with x ; this is consistent with previous studies. The damage appears to accumulate at lower doses deeper in the layer in all alloys. This effect is perhaps most pronounced in $\text{Al}_{0.85}\text{Ga}_{0.15}\text{As}$ where amorphous material initiates at the deeper interface and then proceeds upward through the layer. In $\text{Al}_{0.85}\text{Ga}_{0.15}\text{As}$ the material ahead of the advancing layer does not appear to be damaged, even at the higher doses. This behavior is different than in the lower Al alloys, in which damage appears to accumulate throughout the layer, although at a faster rate deeper in the layer.

Following warm-up the analysis was repeated and a comparison of the spectra at 77 K and 293 K was made for each alloy and at different ion doses in Figures 2 and 3d-f. The spectra at 77 K and 293 K for $\text{Al}_{0.6}\text{Ga}_{0.4}\text{As}$, $\text{Al}_{0.7}\text{Ga}_{0.3}\text{As}$, and $\text{Al}_{0.8}\text{Ga}_{0.2}\text{As}$ are different in that the channeling yield is lower at 293 K than at 77 K. This decrease in the channeling yield indicates that the damage structure has recovered as the sample warms to room temperature. At the highest doses, when the *entire* channeling yield at 77 K is coincident with that of the random, no recovery occurs on warmup. However, when only *part* of the spectrum coincides with the random, recovery is even observed at depths that appeared amorphous to RBS at 77 K (cf. Figures 2a, 2d). Recovery, then, occurs only when a continuous amorphous layer has not been formed, and such an amorphous layer is stable against warmup. In contrast to the $\text{Al}_{0.6}\text{Ga}_{0.4}\text{As}$ results, in $\text{Al}_{0.85}\text{Ga}_{0.15}\text{As}$, no apparent recovery is seen in the RBS spectra as the sample is warmed to room temperature even at low ion doses. Note that this does not necessarily preclude recovery; it only says that the depth resolution of RBS may be insufficient to detect it.

The damage structure corresponding to the room temperature channeling spectra was studied by transmission electron microscopy. An example of the damage structure in $\text{Al}_{0.85}\text{Ga}_{0.15}\text{As}$ is shown in Figure 4 and can be compared with the structure shown in Figures 2a-c, which are from $\text{Al}_{0.6}\text{Ga}_{0.4}\text{As}$ [6]. In contrast to the $\text{Al}_{0.6}\text{Ga}_{0.4}\text{As}$ where some form of damage is observed throughout the layer, the upper portion of $\text{Al}_{0.85}\text{Ga}_{0.15}\text{As}$ shows no structural damage (Figure 4a), although local variations in contrast are observed. The nature of this contrast difference is not known but one possibility is compositional disorder. Separating the undamaged material from the amorphous layer is a band of planar defects that is 20-30 nm wide (Figure 4b). The microstructures observed in both alloys can be used to understand the room temperature channeling spectra. The presence of planar defects in the crystalline layer in $\text{Al}_{0.6}\text{Ga}_{0.4}\text{As}$ is consistent with the observed recovery; it is not likely that the observed recovery is a consequence of

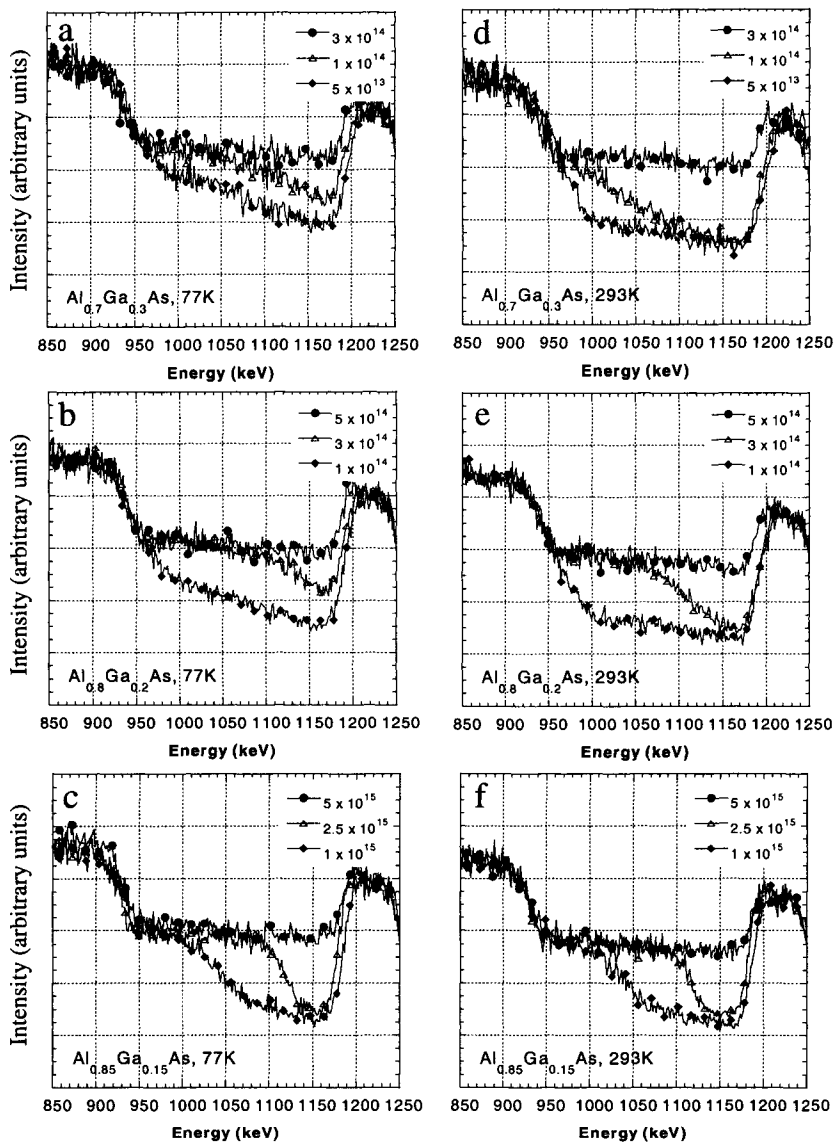


Figure 3: Comparison of implanted samples containing (a,d) Al_{0.7}Ga_{0.3}As, (b,e) Al_{0.8}Ga_{0.2}As, and (c,f) Al_{0.85}Ga_{0.15}As implanted at 77 K with 1.5 MeV Kr to doses shown. Fig a-c show spectra collected at 77 K, d-f show spectra recorded after samples had warmed to room temperature. In all cases, the highest dose shown was the lowest dose to entirely coincide with the random spectrum.

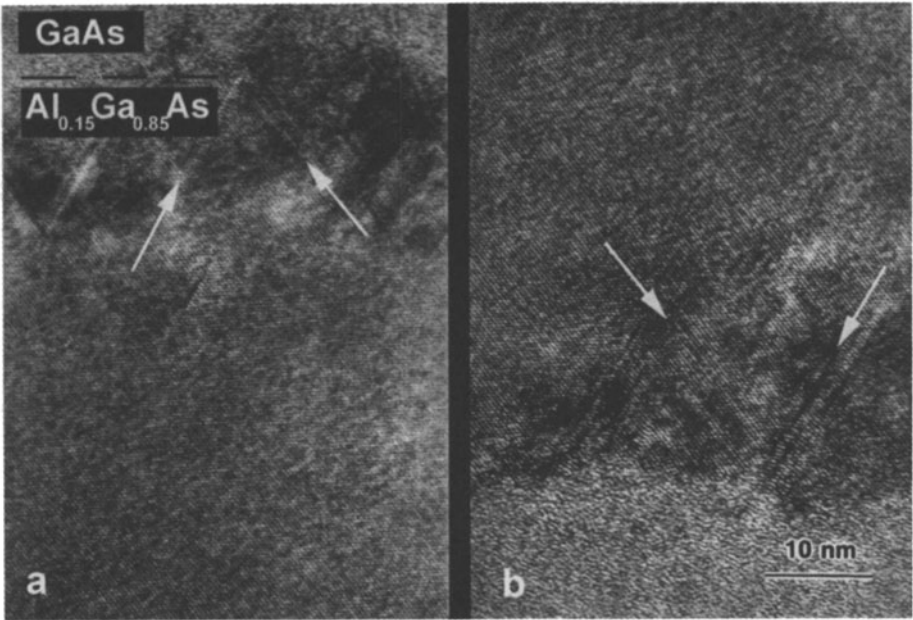


Figure 4: High-resolution TEM image of $\text{Al}_{0.85}\text{Ga}_{0.15}\text{As}$ sample implanted to $5 \times 10^{16} \text{ ions cm}^{-2}$. Left image (a) is of upper GaAs/ $\text{Al}_{0.85}\text{Ga}_{0.15}\text{As}$ interface, right image (b) is from crystalline-to-amorphous boundary. From ref. [7].

annealing of point defects, as, under this implantation condition, dislocation loops are not visible in the recovered microstructure. The origin of the planar defects is less certain in $\text{Al}_{0.85}\text{Ga}_{0.15}\text{As}$, as the width of the defective band is narrower than the resolution of RBS, but planar defects are consistent with recovery of a highly damaged region upon warming from 77 K to room temperature.

In an attempt to observe the evolution of damage as a function of dose and to ascertain the role (if any) of planar defects in the amorphization process, electron transparent cross-sectional TEM samples containing layers of $\text{Al}_{0.6}\text{Ga}_{0.4}\text{As}$ or $\text{Al}_{0.85}\text{Ga}_{0.15}\text{As}$ were implanted at 50 K *in-situ* in the IVEM-Accelerator facility at Argonne National Laboratory [12]. By using this facility, the damage evolution can be observed at the implantation temperature (albeit in a thin foil rather than in a bulk sample). In order to best simulate the effect of an implantation into a bulk sample, which includes mixing at the interface, the samples were tilted 45° with respect to the ion beam and oriented such that the ions penetrated through the $\text{Al}_x\text{Ga}_{1-x}\text{As}$ / GaAs interface.

The micrographs presented in Figure 5 show the damage produced by implantation with 500 keV Kr to a dose of $1.5 \times 10^{14} \text{ ions cm}^{-2}$ in $\text{Al}_{0.6}\text{Ga}_{0.4}\text{As}$ at 50 K (Figure 5a) and after warming to room temperature (Figure 5b). At low temperature only amorphous regions are evident, whereas after warmup planar defects (arrows) and amorphous regions are observed. Although not quantified, the density of planar defects at room temperature appears higher at the interface than away from it. In $\text{Al}_{0.85}\text{Ga}_{0.15}\text{As}$,

Cambridge University Press

978-1-107-41378-8 - Materials Research Society Symposium Proceedings: Volume 540:

Microstructural Processes in Irradiated Materials

Editors: Steven J. Zinkle, Glenn E. Lucas, Rodney C. Ewing and James S. Williams

Excerpt

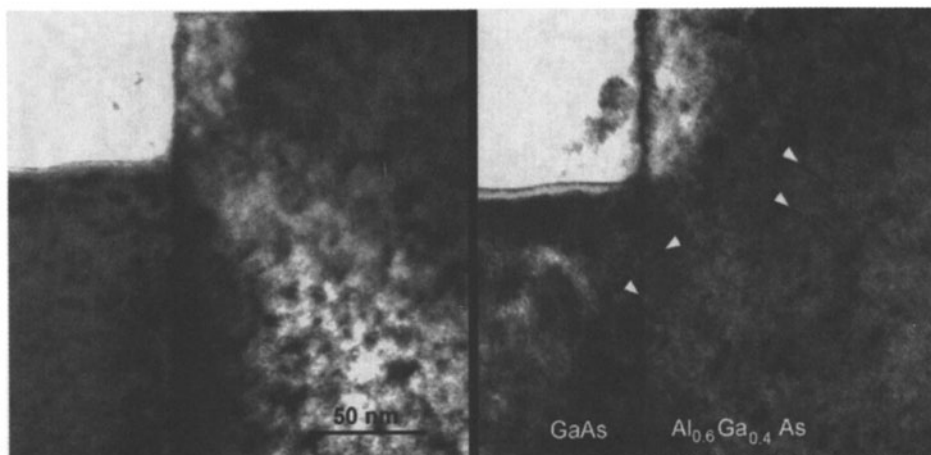
[More information](#)

Figure 5: TEM images of 60 implanted with 500 keV in-situ at 50 K. a) at 50 K, b) after warm-up to room temperature. Arrows indicate planar defects formed during warmup.

amorphous regions and planar defects coexisted at the implantation temperature, but planar defects were neither associated with the amorphous material, nor did the amorphous zones possess the oblong character or the orientation of planar defects. After warmup, planar defects and amorphous material still existed. A higher density of planar defects appeared in the layer than before warmup, again with a higher density at the interface. The formation of planar defects could not be correlated with the removal of any amorphous material, which shows that they do not necessarily form during recrystallization of amorphous material.

At first sight these *in-situ* experiments appear contradictory in that planar defects and amorphous material coexist at the implantation temperature in $\text{Al}_{0.85}\text{Ga}_{0.15}\text{As}$, but not in $\text{Al}_{0.6}\text{Ga}_{0.4}\text{As}$. However, it was discovered that the total damage produced during implantations that were periodically interrupted (as they must be to examine the damage) was less than that produced by a continuous implantation. This was corroborated by experiments using GaAs samples; exposure to the electron beam was minimized for these samples (2-3 minutes maximum). The uninterrupted implant created a considerably higher damage density than the interrupted implant. This effect is, however, a consequence of using an electron transparent foil, which has a typical thickness less than 200 nm; the same effect was not observed in bulk samples. Apparently some recovery or relaxation process can occur in thin foils at 50 K. However, it is known that no defects are mobile in *bulk* implanted GaAs and AlAs until temperatures greater than 200 K [8-11]. Another thin foil effect was seen by Turkot [13], who reported that amorphous material in TEM samples prepared from bulk specimens is not stable at room temperature; over time, the amorphous material converts to randomly oriented crystals that are highly twinned. Bulk implanted samples exposed to the same temperature environment showed no evidence of such recrystallization. All of these observations complicate the interpretation of the results from the implantation of thin foils.

The *in-situ* implantations of electron transparent material do not provide evidence for or against planar defects acting as precursors in the amorphization process, although amorphous regions are not connected